ROYAL SOCIETY OF CHEMISTRY

EDGE ARTICLE

Check for updates

All publication charges for this article have been paid for by the Royal Society of Chemistry

Establishing PQ-ERA photoclick reactions with unprecedented efficiency by engineering of the nature of the phenanthraquinone triplet state†

Youxin Fu, [a] Georgios Alachouzos, [a] Nadja A. Simeth, [‡a] Mariangela Di Donato, [bc] Michiel F. Hilbers, [d] Wybren Jan Buma, [*de] Wiktor Szymanski [*af] and Ben L. Feringa [*a]

The light-induced photocycloaddition of 9,10-phenanthrenequinone (**PQ**) with electron-rich alkenes (**ERA**), known as the **PQ-ERA** reaction, is a highly attractive photoclick reaction characterized by high selectivity, external non-invasive control with light and biocompatibility. The conventionally used **PQ** compounds show limited reactivity, which hinders the overall efficiency of the **PQ-ERA** reaction. To address this issue, we present in this study a simple strategy to boost the reactivity of the **PQ** triplet state to further enhance the efficiency of the **PQ-ERA** reaction, enabled by thiophene substitution at the 3-position of the **PQ** scaffold. Our investigations show that this substitution pattern significantly increases the population of the reactive triplet state ($^3\pi\pi^*$) during excitation of 3-thiophene **PQs**. This results in a superb photoreaction quantum yield (Φ_P, up to 98%), high second order rate constants (k_2, up to 1974 M^{-1} s^{-1}), and notable oxygen tolerance for the **PQ-ERA** reaction system. These results have been supported by both experimental transient absorption data and theoretical calculations, providing further evidence for the effectiveness of this strategy, and offering fine prospects for fast and efficient photoclick transformations.

1. Introduction

The use of photochemical activation[1] procedures in click chemistry reactions has resulted in the emergence of a novel category of light-induced click reaction referred to as "photoclick chemistry".[2,3] As opposed to conventional click reactions, in which the level of spatial and temporal control over the reaction is often limited,[4,5] photochemical reactions provide a high degree of both spatial and temporal control over the reaction, allowing it to occur precisely when needed.[1] The photo-induced cycloaddition of tetrazole and alkene, reported by Lin and co-workers[6] marked the beginning of a decade of significant advancements and since then various types of photoclick reactions have been explored.[7–13] The advantages associated with photoclick reactions, including their temporal and spatial control, non-invasive use of light, high efficiency, and compatibility with various biological systems, make these transformations particularly well-suited for a broad range of applications. These include, but are not limited to, surface modification,[14–16] 3D printing,[17,18] protein labeling,[13,19,20] and bioimaging.[11,21,22]

Among these photoclick reactions, the **PQ-ERA** reaction, originally developed by Schönberg and co-workers in the 1940s,[23,24] is gaining significant attention due to its excellent kinetics and biocompatibility.[11–13] This reaction involves photoinduced electron transfer (PeT) between an electron-rich alkene and a **PQ**, resulting in the formation of a 1,6-biradical intermediate that rapidly undergoes intramolecular radical recombination to form [4 + 2] cycloadducts.[13] Recently we identified new functionalization handles and showed that using enamines as **ERA**s significantly enhances the reaction rate (up to 674 M^{-1} s^{-1}) and photoreaction quantum yields (Φ_P, up to 65%).[12] Despite these advances, further improvement is necessary, in particular regarding efficiency and rate, to expand the

aCentre for Systems Chemistry, Stratingh Institute for Chemistry, Faculty for Science and Engineering, University of Groningen, Nijenborgh 4, 9747 AG Groningen, The Netherlands. E-mail: b.l.feringa@rug.nl

bLENS (European Laboratory for Non-Linear Spectroscopy), Via N. Carrara 1, 50019 Sesto Fiorentino (FI), Italy

cICCOM-CNR, Via Madonna del Piano 10, 50019 Sesto Fiorentino (FI), Italy

dVan 't Hoff Institute for Molecular Sciences, University of Amsterdam, Science Park 904, 1098 XH Amsterdam, The Netherlands. E-mail: W.J.Buma@uva.nl

eInstitute for Molecules and Materials, FELIX Laboratory, Radboud University, Toernooiveld 7c, 6525 ED Nijmegen, The Netherlands

fDepartment of Radiology, Medical Imaging Center, University of Groningen, University Medical Centre Groningen, Hanzeplein 1, 9713 GZ Groningen, The Netherlands. E-mail: w.szymanski@umcg.nl

applicability of this reaction in diverse fields such as material science, bioimaging, and bioconjugation. However, engineering photoactive molecules to modulate excited state properties remains highly challenging.

The mechanism of the **PQ-ERA** reaction involves photoexcitation of **PQ** with UV to blue light, resulting in population of the strongly allowed S_2 ($^1\pi\pi^*$) state, which undergoes internal conversion to the lowest excited S_1 ($^1n\pi^*$) singlet state. An almost quantitative intersystem crossing (ISC) process then takes place, leading to population of the two lowest triplet states, T_1 ($^3\pi\pi^*$) and T_2 ($^3n\pi^*$) (the former being the reactive state for the **PQ-ERA** reaction), which are close in energy.[25–27] This is then followed by a [4 + 2] photocycloaddition reaction with an **ERA**.[28] Thus, a better understanding of the properties of the **PQ**'s triplet state and generating more $^3\pi\pi^*$ triplet states is crucial for further optimization of the **PQ-ERA** photoclick reaction. Recent studies have been conducted showing that triplet energy levels can be influenced by substituents on the aromatic ring and in some aromatic ketones they can even be inverted. This phenomenon is known as "electronic state switching", and it modifies the electronic character of the lowest triplet state, thereby affecting its reactivity.[29–31]

Building on this phenomenon, we present herein a strategy for boosting the reactivity of the triplet state of **PQ** via a simple thiophene substitution at the 3-position of the **PQ** scaffold (Scheme 1) to achieve an unprecedented enhancement of the efficiency of the **PQ-ERA** reaction. Our investigation shows that the thiophene substitution significantly increases the population of the reactive triplet state ($^3\pi\pi^*$) upon excitation of 3-thiophenyl **PQ**s, which then results in a higher photoreaction quantum yield (up to a remarkable value of 98%), higher second order rate constants (up to 1974 M^{-1} s^{-1}), and notable oxygen tolerance for the **PQ-ERA** reaction system. These findings have been supported by both transient absorption experiments and theoretical calculations.

2. Results and discussion

### 2.1 Synthesis and photophysical evaluation of PQ derivatives

Based on our previous study,[12] we assembled the two target compounds from commercially available 3-bromophenanthrene-9,10-dione (**PQ-3Br**), 3,6-dibromophenanthrene-9,10-dione (**PQ-3DiBr**), and thiophene boronic acid in a Suzuki–Miyaura cross-coupling reaction.[32]

Employing palladium-mediated cross-coupling and introducing the substituents via an arene extension, rather than by direct modifications on the **PQ** core, is synthetically straightforward and tolerates a broad set of substrates using the same protocol. We thus obtained **PQ-3TP** and **PQ-3DiTP** in satisfying yields (55% and 39%, respectively, Scheme S1, ESI†) employing Pd(PPh$_3$)$_4$ as catalyst.

Next, both target molecules were characterized in terms of their electronic properties. Analysis of the UV-Vis absorption spectra of both the 3-thiophene and the 3,3′-dithiophene extended **PQ**s revealed that the energetically lowest transition maximum, λ_{max}, lies around 390 nm (Fig. S13†) and is hypsochromically shifted compared to unsubstituted **PQ** (λ_{max} = 410 nm). This band is typically used to excite **PQ** derivates to trigger a **PQ-ERA** photoclick reaction.[12]

2.2 Photoclick reaction kinetics of PQs with PY

To test the performance of the newly synthesized **PQ** derivatives in a [4 + 2] photocycloaddition reaction, we irradiated a solution of each **PQ** (50 μM, MeCN, N$_2$) with a 390 nm LED in the presence of a suitable reaction partner (Fig. 1A and B). We selected N-boc-2,3-dihydro-1H-pyrrole (**PY**, 10 eq., Fig. 1) as the **ERA**, as this cyclic enamine had shown the highest reactivity in our previous study.[12] The progress of the reaction was monitored with UV-Vis spectroscopy providing the experimental rate constants $k_{obs}(390)$ of the photoclick process (0.25 s^{-1} and 0.295 s^{-1} for **PQ-3TP** and **PQ-3DiTP**, respectively, for detailed information see ESI, Section 4.2, Fig. S15 and S16†), which was significantly (>40 times) higher compared to the unsubstituted **PQ_PY** system (0.0062 s^{-1}, Fig. S14†) under the same conditions. Next, we explored whether the system could also be triggered using light with a longer wavelength, since the absorption spectrum of thiophene-substituted **PQ**s features a broad band ranging from 350 nm to 500 nm. We irradiated the **PQs_PY** mixtures with light of different wavelengths (365, 390, 420, and 445 nm) and, as expected, observed in all cases the formation of the photoclick products (Fig. S14–S16†). Important to notice is that the 3-position thiophene substituted **PQ**s led to higher rate constants compared with the unsubstituted **PQ** under the same conditions (for detailed information see ESI, Section 4.2, Fig. S14–S16†). Finally, recognizing that thiophenes are known to be susceptible to side reactions, such as oxidation to radical cations in oxygenated solvents under prolonged light exposure,
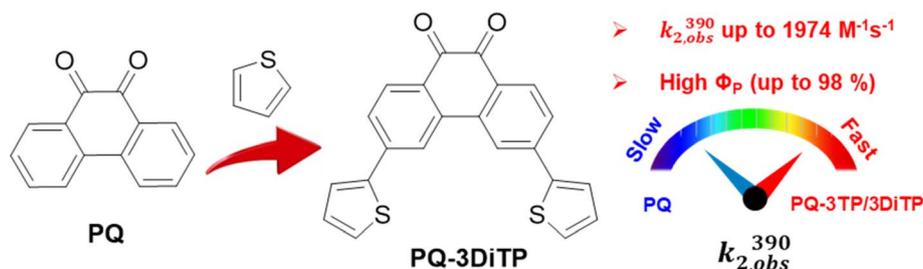
Scheme 1 Comparison of photocycloaddition of 9,10-phenanthrenequinone (**PQ**) with electron-rich alkenes (**ERAs**). $k_{2,obs}(390)$ observed second-order reaction rate; and Φ_P: photoreaction quantum yield.
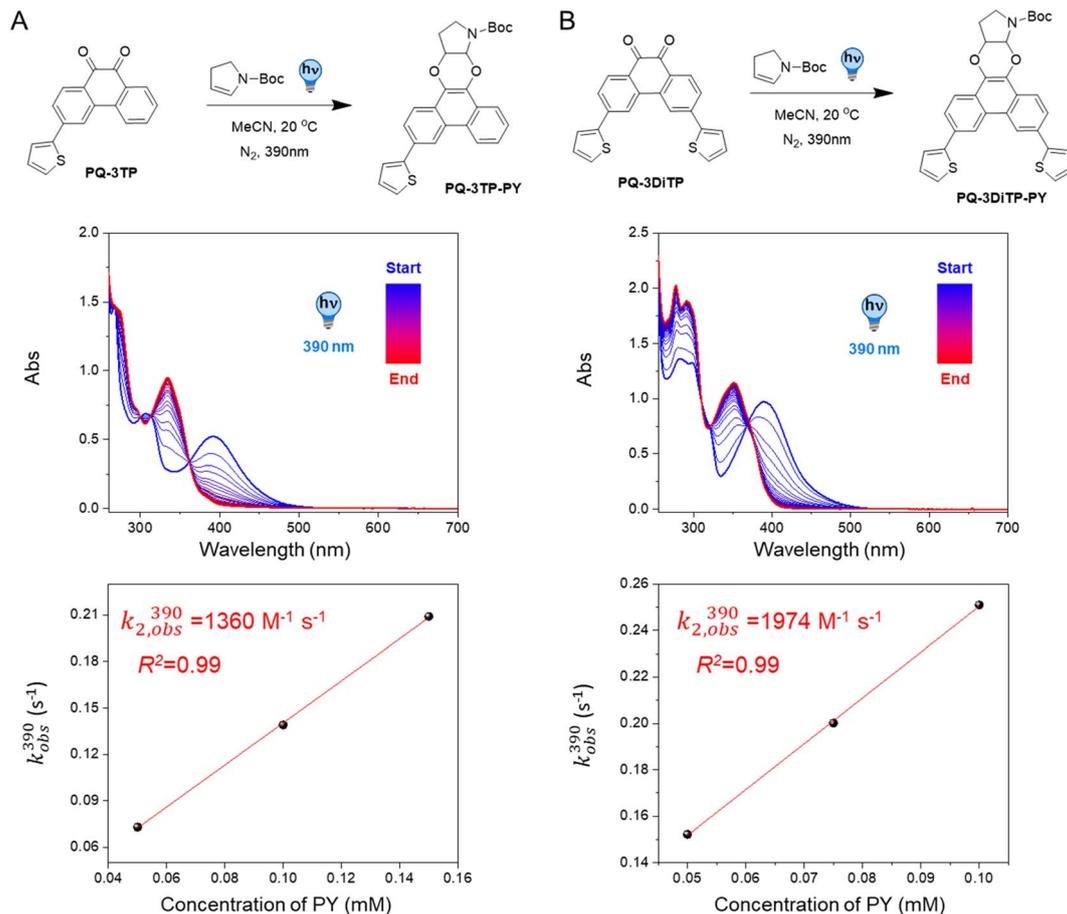
Fig. 1 Kinetic analysis of **PQ-ERA** photocycloadditions. Reaction scheme, time-resolved UV-Vis absorption spectra, and plot of $k_{obs}(390)$ vs. **PY** concentration of (A) **PQ-3TP** (one of the possible isomers formed is shown as an example) and (B) **PQ-3DiTP** towards **PY**. For time-resolved UV-Vis absorption spectra, samples were irradiated by 390 nm LED under N_2 atmosphere at 20 °C. The reaction was followed by UV-Vis absorption spectroscopy (sample interval 1 s, concentration: 50 μM **PQ**s, 500 μM **PY**). The second-order rate constant $k_{2,obs}(390)$ were determined to be 1360 M^{-1} s^{-1} and 1974 M^{-1} s^{-1} for the **PQ-3TP_PY** and **PQ-3DiTP_PY** system, respectively, based on the slope of the fitted line.

we assessed the **PQ-ERA** reaction substrate and product stability using the **PQ-3TP_PY** system as a representative model. We conducted the reaction in the presence of air with extended light irradiation lasting over 15 minutes. Gratifyingly, HPLC analysis revealed a clean reaction (Fig. S24†), strongly supporting the high selectivity of the reaction.

Next, we determined the second-order reaction rate $k_{2,obs}(390)$ of these photocycloaddition reactions (for details and further considerations see ESI Section 4.2, Fig. S17–S19†). The $k_{2,obs}(390)$ was found to be 1360 M^{-1} s^{-1} and 1974 M^{-1} s^{-1} for **PQ-3TP_PY** and **PQ-3DiTP_PY**, respectively (Fig. 1), which is more than 11 600 times higher than for the original **PQ-VE1** (ethylene glycol vinyl ether) system (0.117 M^{-1} s^{-1})[12] and over 160 times higher than the **PQ–PY** system (8.2 M^{-1} s^{-1}, Fig. 2B and S17, for detailed information see ESI, Section 4.2†) under the same reaction conditions. In fact, this allows us to perform quantitative photoclick reactions in a matter of seconds. As such, it represents the fastest currently known **PQ-ERA** photoclick reaction.[11–13]

Furthermore, in order to evaluate the generality of our 3-position thiophene substitution approach, we selected two

additional **ERA**s, 4-oxo-3,4-dihydropyridine-1(2H)-carboxylate (**PYD**) and 3,4-dihydro-2H-pyran (**DP**), to react with both **PQ** and **PQ-3TP**. Analysis of the kinetic traces acquired through UV-Vis absorption spectroscopy (for details and further considerations see ESI Section 4.2, Fig. S20 and S21†) revealed that the photoclick reaction was significantly more efficient in the **PQ-3TP** system when compared to the **PQ** system. Specifically, under 390 nm light irradiation, the **PQ-3TP** system displayed $k_{obs}(390)$ values of 0.0059 s^{-1} and 0.092 s^{-1} for **DP** and **PYD**, respectively, whereas the **PQ** system exhibited $k_{obs}(390)$ values of 0.0003 s^{-1} and 0.0028 s^{-1} for **DP** and **PYD**, respectively. Finally, to evaluate if heteroaromatic compounds with a lower aromatic stabilization energy are able to work as **ERA**s in this reaction, we conducted reaction between **PQ-3TP** and an aromatic compound, specifically **1-methylindole**, under the same conditions. As depicted in Fig. S22 (ESI, Section 4.2),† minimal changes were observed over a 15 minute period, indicating the absence of photoclick reactions between **PQ-3TP** and **1-methylindole** upon 390 nm light irradiation, showing a general limitation of the electronic properties of **ERA**s in this reaction system. These findings serve as further evidence that
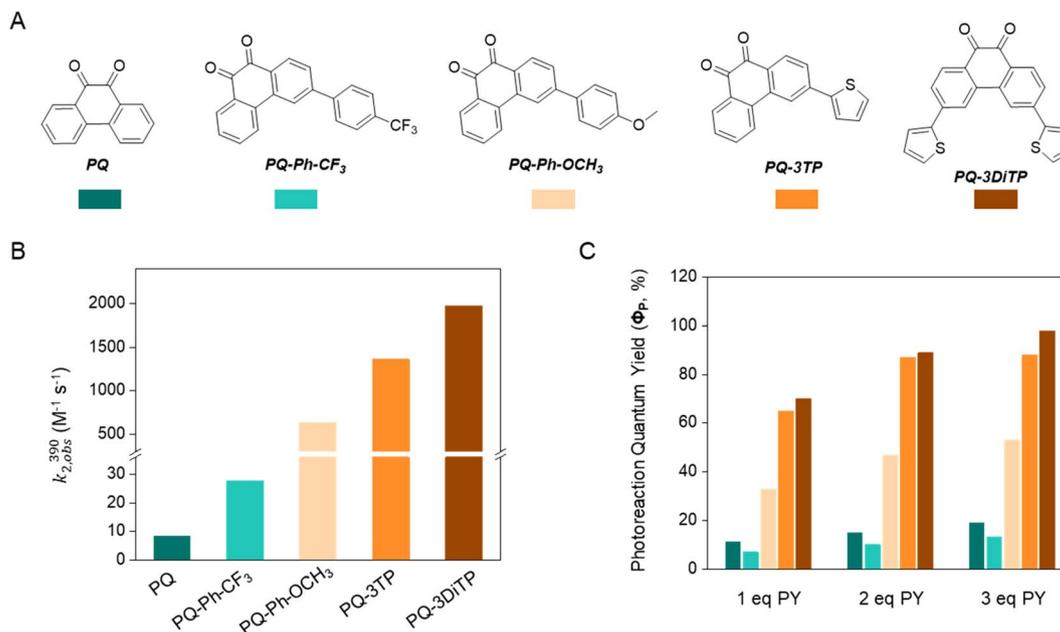
Fig. 2 Overview of the second order reaction rate (k_2) and photoreaction quantum yield (Φ_P) of the **PQ-ERA** photoclick reaction system. (A) Structures of the investigated **PQ**s, (B) $k_{2,\text{obs}}(390)$ and (C) Φ_P of **PQ-ERA** photoclick reaction.

the 3-position thiophene substitution strategy can enhance the photoclick reactivity of **PQ** towards a variety of **ERA**s.

These results are mirrored by the extraordinary high photoreaction quantum yield (Φ_P) of these **PQ-ERA** reactions, which has been determined for reactions of **PQ**, **PQ-Ph-CF₃**, **PQ-Ph-OCH₃**, **PQ-3TP**, and **PQ-3DiTP** with different concentrations of **PY** (Fig. 2A). **PQ-3TP** and **PQ-3DiTP** exhibited an extremely high value of Φ_P, reaching the up to 98% in the presence of 3 eq. of **PY** (Fig. 2C, for detailed information, see ESI, Section 4.3†). To the best of our knowledge, this is the highest Φ_P observed for any photoclick reaction reported so far.[3,12,33–36] Thus, the performance of the 3-position thiophene substituted **PQ-3TP/PQ-3DiTP_PY** system is markedly enhanced compared to our previously introduced **PQs-VEs/PY** systems ($\Phi_{P(\text{PQs-VEs/PY})}$ ranging from 0.6%[12] to 53%, for details and further considerations see ESI Section 4.3, Fig. S25–S39†) as well as other reported photoclick reactions such as, for instance, *o*-naphthoquinone methides (*o*NQMs)-ene hetero-Diels–Alder cycloaddition ($\Phi_P = 20\%$),[36] photoinduced tetrazole–alkene cycloaddition ($\Phi_P = 0.29\%$ to 24%),[22,35] and photoinduced sydnone–alkene/alkyne cycloadditions ($\Phi_P = 10\%$ to 25%).[33,34]

2.3 Effect of O₂ and temperature on the PQ-ERA photoclick reaction

The photochemical characterization of the thiophene-**PQ-ERA** reaction reported so far shows that both **PQ-3TP** and **PQ-3DiTP** react significantly faster with **PY** compared to unsubstituted **PQ** and other **PQ** derivatives (Fig. 2B). Thus, we chose **PQ-3TP** as an ideal candidate to conduct a systematic and detailed study on the **PQ-ERA** photoclick reaction process (Fig. 3A). Previous reports showed that irradiation of **PQ**s with

390 nm light in the presence of **ERA**s proceeds *via* the triplet state of **PQ**s and results in the photocycloaddition of the two reactants, furnishing the **PQ-ERA** products.[13,27,28] We examined the effect of molecular oxygen (O₂), an important triplet state quencher,[37,38] on the **PQ-ERA** reaction process.[11] To probe the effect that O₂ had on the **PQ-ERA** photocycloaddition, we sought to determine the $k_{\text{obs}}(390)$ of the **PQ-3TP_PY** photoclick reaction under both deoxygenated and non-deoxygenated conditions. As expected, in the absence of oxygen we found a higher $k_{\text{obs}}(390)$ compared to the non-degassed solutions ($0.084 \rightarrow 0.229$ s⁻¹ and $0.014 \rightarrow 0.092$ s⁻¹ respectively, Fig. 3B), demonstrating the detrimental effect of O₂ on this **PQ-ERA** reaction and corroborating the hypothesis of the involvement of triplet states. Nonetheless, our results indicate that, contrary to previous **PQ-ERA** photoclick systems,[12] the **PQ-3TP_PY** photoclick reaction still proceeds also under aerobic conditions, marking an overall improvement in oxygen tolerance.

Also, previous studies have demonstrated that lowering the temperature may result in a prolonged triplet lifetime.[39–41] Based on this, we hypothesized that changes in temperature would also have an effect on the **PQ-3TP_PY** photoclick reaction. To investigate this effect, the photoclick reactions were conducted over a temperature range between 0 °C to 50 °C, monitoring the reactions using UV-Vis spectroscopy to measure the experimental rate constants $k_{\text{obs}}(390)$ of the photoclick process. As shown in Fig. 3C, a clear enhancement of the photoclick reactivity was observed at lower temperatures. On the basis of quantum chemical calculations that will be discussed below, we attribute this enhancement to a reduced non-radiative decay rate of the reactive triplet state at lower temperatures leading to a longer lifetime.[39,42]
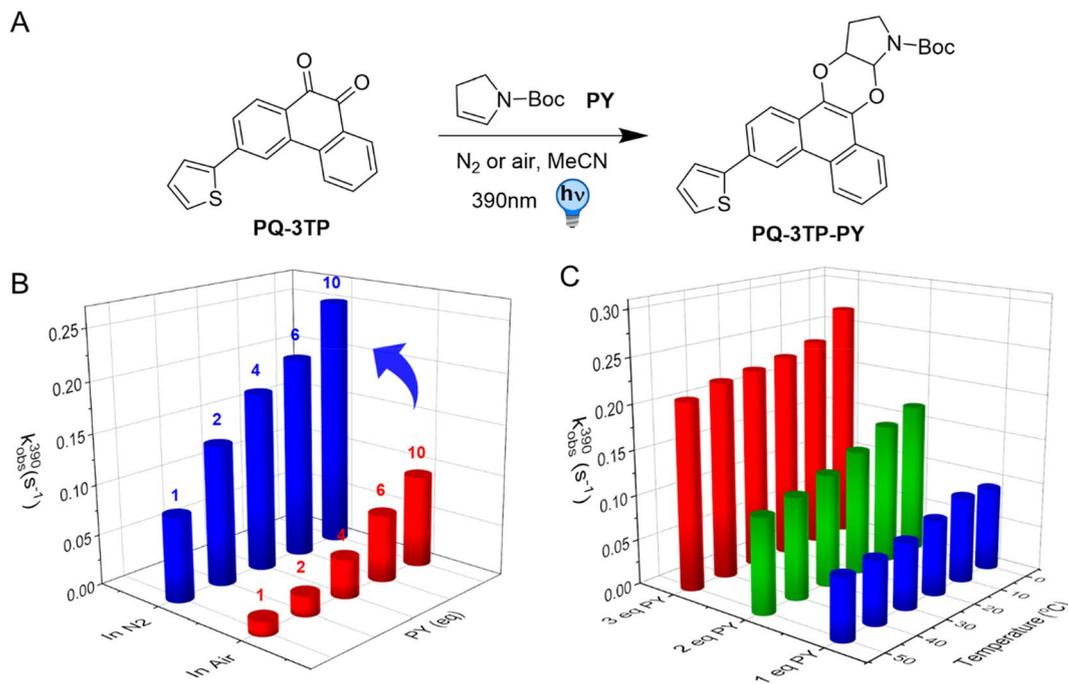
Fig. 3 Kinetic analysis of **PQ-3TP_PY** photoclick reaction. (A) Reaction scheme (one of the possible isomers formed is shown as an example), (B) kinetic analysis of photocycloaddition between **PQ-3TP** (50 μM) with varying amounts of **PY** (1, 2, 4, 6, and 10 eq.) addition under both N_2 (blue cylinders) and air (red cylinders) atmosphere at 20 °C. (C) Temperature dependence kinetic analysis of **PQ-3TP_PY** photoclick reaction in MeCN under different temperature 0 °C, 10 °C, 20 °C, 30 °C, 40 °C, and 50 °C respectively. For all of the measurements, the sample was irradiated with a 390 nm LED and followed over time by UV-Vis absorption spectroscopy (1 cm cuvette, 2.5 mL MeCN sample volume, sample interval 1 s).

The results shown above indicate that the 3-position thiophene substitution on the **PQ** scaffold can bring about a marked improvement in its photoclick reactivity and that oxygen can be tolerated in the systems. Aerobic conditions result in slower photoclick reaction rates, but still allow the completion of the model reaction in less than two minutes. To gain a further fundamental understanding of these new phenomena, we next performed a detailed study on the electronically excited singlet and triplet states of **PQ**s and their excited-state dynamics using femtosecond/nanosecond transient absorption spectroscopy and quantum chemical calculations.

2.4 Femtosecond/nanosecond transient absorption spectroscopy

We initially hypothesized that the improved reactivity of the 3-thiophene substituted **PQ**s could in principle be attributed either to a higher triplet quantum yield or to a longer-lived triplet state. To further investigate the excited state dynamics of the newly synthetized **PQ**s, the transient absorption spectra of these systems were measured both in the sub-picosecond to nanosecond and nanosecond to millisecond timescale. Previous studies demonstrated that unsubstituted **PQ** undergoes a rapid ISC, producing triplet states with a high
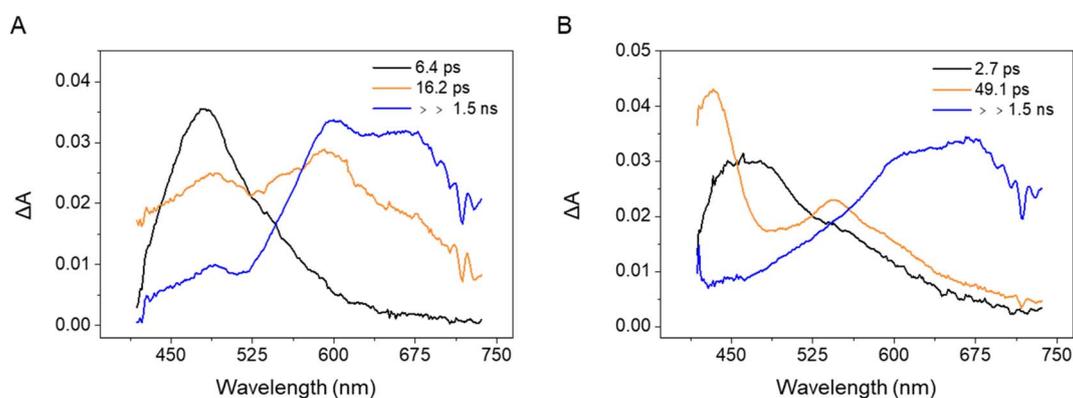

Fig. 4 EADS obtained from a global analysis of the transient absorption data recorded for (A) **PQ-3TP** and (B) **PQ-3DiTP** in MeCN upon excitation at 400 nm.

quantum yield.[29,43] The triplet absorption spectrum reported for **PQ** presents two positive bands at about 460 and 650 nm that have been attributed to two different triplet states with $^3n\pi^*$ and $^3\pi\pi^*$ nature reaching a fast equilibration.[29]

Our measurements confirmed the occurrence of very fast ISC for **PQ**: indeed, upon exciting the molecule with 400 nm light, the transient spectrum attributed to the triplet state rises in about 9 ps. The decay of the absorption spectrum, as determined by ns transient absorption spectroscopy, is bi-exponential, with a major component decaying in 1.47 μs and a residual component with a lifetime of 40.5 μs (Fig. 5A, for detailed information, see ESI, Section 4.4 and 4.5, Fig. S40, S41 and S44†).

The transient absorption measurements were then repeated for the 3-substituted samples **PQ-3TP** (Fig. S42A†) and **PQ-3DiTP** (Fig. S43A†). Analogous to our analyses of the time-resolved spectra obtained for **PQ**, the recorded transient data have been analyzed using a global fit procedure and employing a sequential linear decay kinetic scheme from which the EADS (Evolution Associated Difference Spectra) and the rate constants describing the excited state dynamics are obtained (for detailed information, see ESI, Section 4.4, Fig. S42 and S43†). The EADS obtained for **PQ-3TP** and **PQ-3DiTP**, which are shown in Fig. 4, are qualitatively similar.

For both systems, the transient spectrum observed directly after excitation features a quite broad positive band peaked at about 470 nm, which, in analogy with observations made for **PQ** (Fig. S40†), can be assigned to excited state absorption (ESA) of the singlet state of the molecules (black EADS in Fig. 4A and B). The spectrum evolves within 6.4 ps in case of **PQ-3TP** to a double peaked structure (orange EADS, Fig. 4A). A further evolution is observed to occur in about 16 ps. On this timescale, the intensity of the band peaked at about 470 nm decays significantly, while a broad band extending from 580 to 700 nm rises in intensity. The lifetime of this spectral component is longer than the time range of the experiment, and, in analogy with what was observed for **PQ**, is assigned to a triplet state. For **PQ-3DiTP**, the initial EADS (Fig. 4B), assigned to a singlet excited state, evolves in about 2.7 ps towards the second component, which is characterized by an intense band at 430 nm and a second less intense band at 550 nm. This EADS then evolves in the final one on a time scale of about 49 ps. The shape of the long-living component for **PQ-3DiTP** is similar to the one observed for **PQ-3TP** and is therefore also assigned to a triplet state. The nature of the intermediate component is not clear: it could be attributed as a high-energy triplet state that rapidly decays into the lower-energy triplet, or to a 'dark' electronically excited singlet state, different from the state that initially is excited. The notable spectral difference between the first and second EADS makes it quite unlikely that the initial evolution is associated with a relaxation process within the state that is initially excited. The rapid evolution between the second
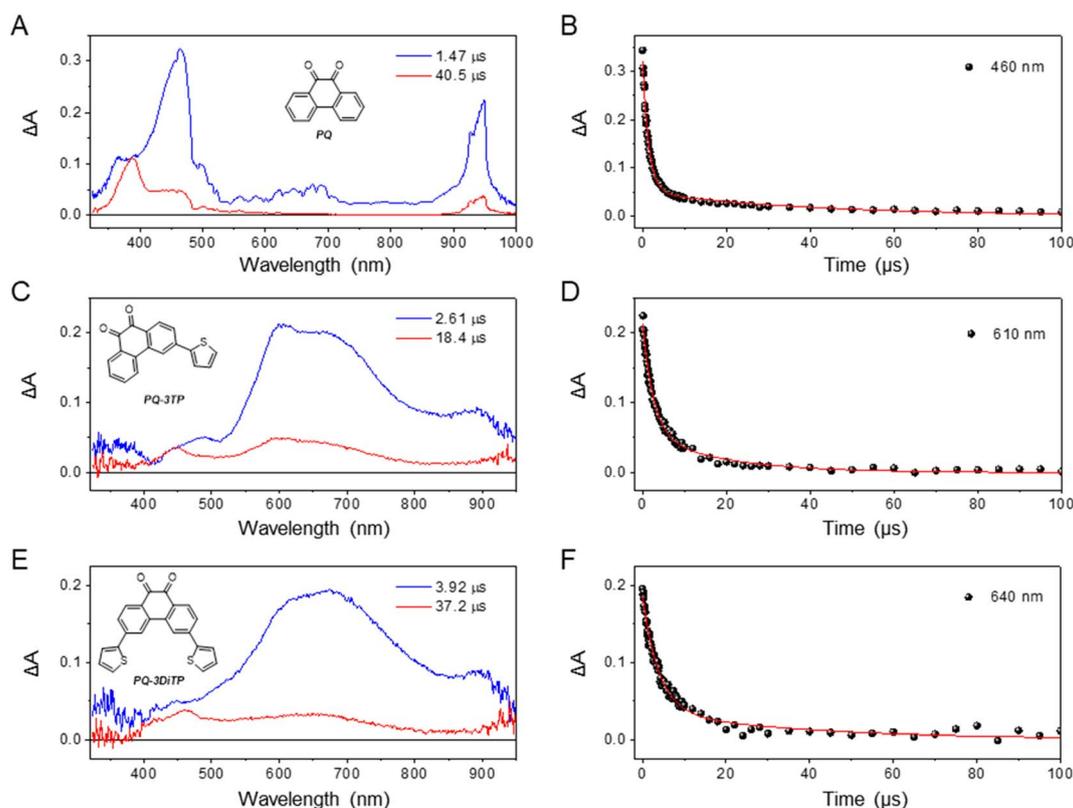

Fig. 5 Evolution-associated difference spectrum (EADS) obtained from global analysis of ns transient absorption data recorded for (A) **PQ**, (C) **PQ-3TP**, and (E) **PQ-3DiTP** in degassed MeCN upon excitation at 400 nm. The fit of the decay of the absorption of the transient signal (red line) (B) **PQ** (at 460 nm), (D) **PQ-3TP** (at 610 nm), and (F) **PQ-3DiTP** (at 640 nm) as obtained from a global analysis of the transient absorption spectra.

and third component suggests that the more likely interpretation for the second EADS is that of a 'dark' singlet state from which ISC occurs. Such a conclusion is fully supported by the results of the quantum chemical calculations discussed below which show that – analogous to **PQ** – the 'bright' state that is excited is the S_2 ($^1\pi\pi^*$) state, while at lower excitation energies the 'dark' S_1 ($^1n\pi^*$) state is found (for detailed information, see the ESI, Section 5†). The ultrafast transient absorption spectra and relevant kinetic traces measured for **PQ-3TP** and **PQ-3DiTP** are shown in Fig. S42 and S43.† The analysis of these traces shows that the band peaked at about 630 nm, which is attributed to the triplet state, rises on a slightly faster timescale for **PQ-3TP**.
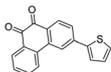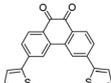
To confirm that the long-living components observed from the ultrafast measurements can be attributed to triplet states, we also measured the transient absorption spectra of both **PQ-3TP** and **PQ-3DiTP** using nanosecond (ns) laser excitation (for detailed information, see ESI, Section 4.5, Fig. S44–S46†). The EADS obtained from global analysis of the data recorded on the longer timescale are reported in Fig. 5, where for comparison also the EADS obtained from the global analysis of the **PQ** ns data are depicted. As can be observed, the spectrum obtained for both **PQ-3TP** and **PQ-3DiTP** immediately after excitation with a ns laser coincides with the long-living species observed in the ultrafast experiments, confirming its assignment in terms of a triplet state of both molecules. Similarly to what is observed for **PQ** (Fig. 5A and B), the triplet state decays bi-exponentially for both compounds with time constants of $\tau_1 = 2.61$ μs (blue component) and $\tau_2 = 18.4$ μs (red component) in case of **PQ-3TP**, and $\tau_1 = 3.92$ μs (blue component) and $\tau_2 = 37.2$ μs (red component) for **PQ-3DiTP**.

Some further comments should be made on these lifetimes. Firstly, only mono-exponential triplet decays have been reported for **PQ** so far. The observation of a bi-exponential decay for all three compounds should thus be rationalized. Secondly, for the ns transient absorption spectra reported for **PQ-3TP** and **PQ-3DiTP** in Fig. 5 and for **PQ** in Fig. S44,† excitation energies in the range of 0.2–0.4 mJ per pulse have been used, which are similar to those employed in previous transient absorption experiments on **PQ**.[29]

For **PQ**, we find indeed a fast decay component ($\tau_1 = 1.5$ μs) that reproduces the previously reported value.[29] However, by repeating the measurements with different excitation energies, we noticed that both lifetimes increase upon lowering the excitation power, suggesting the occurrence of quenching at high irradiation energies. Furthermore, while the long-wavelength band (550–800 nm) is dominated by the fast decay component, the band around 450 nm predominantly decays on the longer time scale. In line with previous studies, we attribute this band to the formation of a ketyl radical, a side reaction product previously identified upon irradiation of **PQ**s.[25–27,44,45] We thus conclude that excitation of **PQ**, **PQ-3TP** and **PQ-3DiTP** leads to population of the lowest triplet state, which decays on a time scale of τ_1, and the formation of a ketyl radical that disappears on a time scale of τ_2. The observed quenching of the triplet is in line with previous studies of **PQ** in acetonitrile in which self-quenching was observed as well,[46] while the disappearance of the ketyl radical is intrinsically bimolecular in nature. Finally, we point out that the triplet lifetimes of all compounds changed in a similar way with the excitation power, remaining on the same order of magnitude among each other. Further information about the power dependence of the triplet lifetimes can be found in the ESI, Section 4.6, Fig. S47–S49.†

Comparison of the blue EADS in Fig. 5 – attributed to the decay of the triplet state – of **PQ** with those of **PQ-3TP** and **PQ-3DiTP** shows significant differences. In the former case, the 400–500 nm band dominates the spectrum with a minor contribution from the broad band system spanning the 600–750 nm region, while for the latter the 400–500 nm band is nearly absent, and the spectrum is dominated by the 550–800 nm band system. This observation strongly suggests a population distribution involving two different triplet states in the three compounds with a different distribution for **PQ** compared to **PQ-3TP** and **PQ-3DiTP**. Such a conclusion nicely explains the differences in the experimentally observed photoclick quantum yield and rate constant (Fig. 2) and leads to the conclusion that the triplet state that is dominantly populated in **PQ-3TP** and **PQ-3DiTP** is much more reactive. In the following we will argue that this triplet state is the $^3\pi\pi^*$ state.

Table 1 Vertical and adiabatic excitation energies of the $^3n\pi^*$ and $^3\pi\pi^*$ states of PQ, PQ-3TP and PQ-3DiTP obtained at the M06-2X/6-31+G*/PCM(acetonitrile) level. Excitation energies in eV, energy differences in kcal mol^{-1}

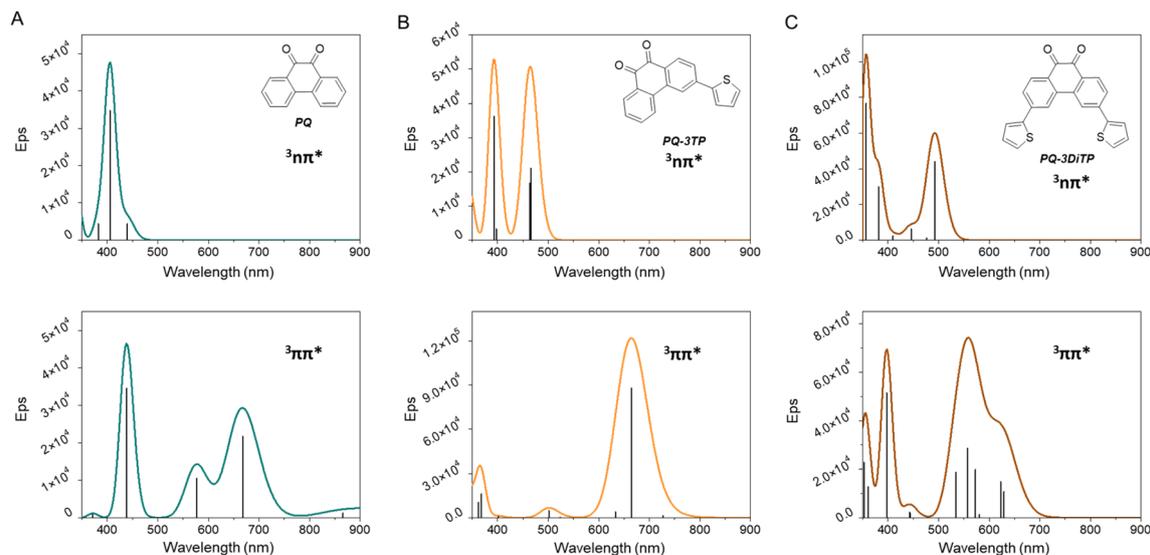|	Structure of **PQs**	$^3\pi\pi^*$ (vertical)	$^3n\pi^*$ (vertical)	$^3n\pi^*$–$^3\pi\pi^*$	$^3\pi\pi^*$ (adiabatic)	$^3n\pi^*$ (adiabatic)	$^3n\pi^*$–$^3\pi\pi^*$
PQ[a]		2.62	2.39	−5.3	2.25 (2.07)[a]	2.34	+2.1 (+2.4)[a]
PQ-3TP		2.40	2.40	−0.4	2.03	2.34	+7.1
PQ-3DiTP		2.51	2.40	−2.6	2.17	2.34	+3.9

[a] Experimental.[53]

Fig. 6 Calculated absorption spectra for the $^3n\pi^*$ (up) to $^3\pi\pi^*$ (down) states of (A) **PQ**, (B) **PQ-3TP** and, (C) **PQ-3DiTP**. Stick spectra have been convoluted with a Gaussian profile with a width of 0.1 eV for further comparison with the experiment.

2.5 Quantum chemical calculations on PQs

To further elucidate the observations made in the transient absorption studies, (Time-Dependent) Density Functional Theory (TD-DFT) calculations have been performed of vertical and adiabatic excitation energies of the lower-lying triplet states as well as of electronic absorption spectra predicted for these states.[47–52] In these calculations, several levels of theory have been employed, giving rise to very similar results. Since the calculations at the M06-2X/6-31+G*/PCM(acetonitrile) level predict for **PQ** a $^3n\pi^*$–$^3\pi\pi^*$ energy gap closest to the value reported experimentally, we will in the following discuss the results obtained at that level. Further details are given in the ESI Section 5.†

Table 1 presents the vertical and adiabatic excitation energies of the lowest $^3n\pi^*$ and $^3\pi\pi^*$ states of **PQ**, **PQ-3TP** and **PQ-3DiTP**. As can be seen, for vertical excitation the $^3n\pi^*$ state is T$_1$, but adiabatically the $^3\pi\pi^*$ state becomes the lowest excited triplet state. Interestingly – and in agreement with the charge distribution and bonding characteristics of the n orbital and of the HOMO and LUMO orbitals – it is observed (i) that the energy of the $^3n\pi^*$ state is hardly changed upon geometry relaxation, while the reorganization energy of the $^3\pi\pi^*$ state is much larger, and (ii) that substitution on the 3 position does not change the vertical and adiabatic excitation energies of the $^3n\pi^*$ state, while the $^3\pi\pi^*$ state is lowered in energy.

The electronic absorption spectra for the $^3n\pi^*$ and $^3\pi\pi^*$ states of **PQ**, **PQ-3TP**, and **PQ-3DiTP** are shown in Fig. 6. These spectra are quite informative, as they predict for **PQ** that the $^3n\pi^*$ state only shows an appreciable absorption around 400 nm, while the $^3\pi\pi^*$ state shows a slightly red-shifted band in the 400 nm region but also strong absorption bands in the 550–750 nm region. Similar observations are made for the predicted absorption spectra of the $^3n\pi^*$ and $^3\pi\pi^*$ states of **PQ-3TP** and **PQ-3DiTP** which only show appreciable absorption above 550 nm for the $^3\pi\pi^*$ state. These observations strongly suggest that the band observed in this region in the experimental transient absorption

spectra of these compounds (Fig. 5) is associated with the $^3\pi\pi^*$ state and not with the $^3n\pi^*$ state as assumed previously.[29] In the ESI Section 5,† we expand further on this difference in conclusions. Based on the current calculations, it is predicted that the short-wavelength band detected in the ns transient absorption experiments can be attributed to absorption from both the $^3n\pi^*$ and $^3\pi\pi^*$ states, whereas the long-wavelength band can only be linked to absorption from the $^3\pi\pi^*$ state. In combination with the calculated adiabatic excitation energies of the two states showing that the $^3\pi\pi^*$ state is lowered in energy upon substitution, we therefore conclude that the photoclick reaction occurs in this state. Such a conclusion finds strong support from studies we have performed on 2,2′-substituted **PQ**s substituted for which the $^3\pi\pi^*$ state is both vertically as well as adiabatically the lowest excited triplet state with the $^3n\pi^*$ state at much higher energies ($\sim$15 kcal mol^{-1}).[54]

Summarizing all the experimental spectroscopic observations and the theoretical calculations, we conclude that in **PQ** and 3-thiophene-extended **PQ**s the following sequence of events occurs. Excitation populates a strongly allowed $^1\pi\pi^*$ state, which undergoes internal conversion on a ps time scale to the lower-lying $^1n\pi^*$ state. Following El-Sayed's rules,[55] this state has a strong spin–orbit coupling with the $^3\pi\pi^*$ state. As a result, a fast and efficient intersystem crossing at a tens of ps timescale occurs that populates the $^3\pi\pi^*$ state, that is the reactive state from which the photoclick reaction occurs. The difference in photoclick quantum yield and rate constant between **PQ** and 3-thiophene extended **PQ**s results from a dominant participation of the $^3n\pi^*$ state in the former.

3. Conclusion

In summary, we report how a simple substitution of the 3- and 3′-position of **PQ**s with either one or two thiophene moieties results in an exceptionally high photoclick quantum yield (up to

98%), higher photoclick rate constants (up to 1974 $M^{-1} s^{-1}$) and marked oxygen tolerance. We have also provided transient absorption data, strongly supporting the suggestion that the appropriate reactive triplet state that engages in the photocycloaddition with **ERA**s is preferentially populated during the excitation of 3-thiophenyl **PQ**s. We envision that this novel ultrafast **PQ-ERA** photoclick reaction with 3-thiophenyl **PQ**s is not limited to the chemistries shown here but will be advantageous in a wide range of applications, such as surface photopatterning, labeling of biomacromolecules, and photochemical crosslinking. Studies along these lines are now ongoing in our laboratories.

Data availability

All experimental and computational data associated with this article have been included in the main text and ESI.†

Author contributions

Y. F., G. A., N. A. S., M. D. D., W. S., W. J. B., and B. L. F. conceived the project and designed phenanthrenequinone derivatives. B. L. F. and W. S. guided the research. Y. F. synthesized all phenanthrenequinone derivatives. G. A. and W. J. B. performed the TD-DFT calculations. Y. F. performed UV-Vis experiments. M. D. D. performed the femtosecond transient absorption spectroscopy measurements. Y. F., M. F. H., and W. J. B. performed the nanosecond transient absorption spectroscopy measurements. Y. F., G. A., N. A. S., M. D. D., W. S., W. J. B., and B. L. F. wrote the manuscript with support and contributions from all authors.

Conflicts of interest

There are no competing conflicts of interests to declare.

Acknowledgements

References

1 M. Montalti, A. Credi, L. Prodi and M. T. Gandolfi, *Handbook of Photochemistry*, CRC Press, 2006.

2 M. A. Tasdelen and Y. Yagci, *Angew. Chem., Int. Ed.*, 2013, **52**, 5930–5938.

3 B. D. Fairbanks, L. J. Macdougall, S. Mavila, J. Sinha, B. E. Kirkpatrick, K. S. Anseth and C. N. Bowman, *Chem. Rev.*, 2021, **121**, 6915–6990.

4 C. W. Tornøe, C. Christensen and M. Meldal, *J. Org. Chem.*, 2002, **67**, 3057–3064.

5 V. V. Rostovtsev, L. G. Green, V. V. Fokin and K. B. Sharpless, *Angew. Chem., Int. Ed.*, 2002, **41**, 2596–2599.

6 W. Song, Y. Wang, J. Qu and Q. Lin, *J. Am. Chem. Soc.*, 2008, **130**, 9654–9655.

7 C. E. Hoyle and C. N. Bowman, *Angew. Chem., Int. Ed.*, 2010, **49**, 1540–1573.

8 A. A. Poloukhtine, N. E. Mbua, M. A. Wolfert, G.-J. Boons and V. V. Popik, *J. Am. Chem. Soc.*, 2009, **131**, 15769–15776.

9 L. Zhang, X. Zhang, Z. Yao, S. Jiang, J. Deng, B. Li and Z. Yu, *J. Am. Chem. Soc.*, 2018, **140**, 7390–7394.

10 C. Stuckhardt, M. Wissing and A. Studer, *Angew. Chem., Int. Ed.*, 2021, **60**, 18605–18611.

11 Y. Fu, H. Helbert, N. A. Simeth, S. Crespi, G. B. Spoelstra, J. M. van Dijl, M. van Oosten, L. R. Nazario, D. van der Born, G. Luurtsema, W. Szymanski, P. H. Elsinga and B. L. Feringa, *J. Am. Chem. Soc.*, 2021, **143**, 10041–10047.

12 Y. Fu, N. A. Simeth, R. Toyoda, R. Brilmayer, W. Szymanski and B. L. Feringa, *Angew. Chem., Int. Ed.*, 2023, **62**, e202218203.

13 J. Li, H. Kong, L. Huang, B. Cheng, K. Qin, M. Zheng, Z. Yan and Y. Zhang, *J. Am. Chem. Soc.*, 2018, **140**, 14542–14546.

14 S. Arumugam, S. V. Orski, J. Locklin and V. V. Popik, *J. Am. Chem. Soc.*, 2012, **134**, 179–182.

15 S. Arumugam and V. V. Popik, *J. Am. Chem. Soc.*, 2012, **134**, 8408–8411.

16 C. Xie, W. Sun, H. Lu, A. Kretzschmann, J. Liu, M. Wagner, H.-J. Butt, X. Deng and S. Wu, *Nat. Commun.*, 2018, **9**, 3842.

17 R. Rizzo, D. Ruetsche, H. Liu and M. Zenobi-Wong, *Adv. Mater.*, 2021, **33**, 2102900.

18 S. J. Bailey, E. Hopkins, K. D. Rael, A. Hashmi, J. M. Urueña, M. Z. Wilson and J. Read de Alaniz, *Angew. Chem., Int. Ed.*, 2023, e202301157.

19 K. Lang, L. Davis, S. Wallace, M. Mahesh, D. J. Cox, M. L. Blackman, J. M. Fox and J. W. Chin, *J. Am. Chem. Soc.*, 2012, **134**, 10317–10320.

20 P. An, T. M. Lewandowski, T. G. Erbay, P. Liu and Q. Lin, *J. Am. Chem. Soc.*, 2018, **140**, 4860–4868.

21 C. Wang, H. Zhang, T. Zhang, X. Zou, H. Wang, J. E. Rosenberger, R. Vannam, W. S. Trout, J. B. Grimm, L. D. Lavis, C. Thorpe, X. Jia, Z. Li and J. M. Fox, *J. Am. Chem. Soc.*, 2021, **143**, 10793–10803.

22 G. S. Kumar, S. Racioppi, E. Zurek and Q. Lin, *J. Am. Chem. Soc.*, 2022, **144**, 57–62.

23 A. Schönberg and A. Mustafa, *Nature*, 1944, **153**, 195.

24 A. Schönberg and A. Mustafa, *J. Chem. Soc.*, 1944, 387.

25 Y. L. Chow and T. C. Joseph, *Chem. Commun.*, 1968, 604.

26 P. A. Carapellucci, H. P. Wolf and K. Weiss, *J. Am. Chem. Soc.*, 1969, **91**, 4635–4639.

27 M. B. Rubin and Z. Neuwirth-Weiss, *J. Am. Chem. Soc.*, 1972, **94**, 6048–6053.

28 J. Li, H. Kong, C. Zhu and Y. Zhang, *Chem. Sci.*, 2020, **11**, 3390–3396.

29 V. R. Kumar, N. Rajkumar, F. Ariese and S. Umapathy, *J. Phys. Chem. A*, 2015, **119**, 10147–10157.

30 K. F. Chang, M. Reduzzi, H. Wang, S. M. Poullain, Y. Kobayashi, L. Barreau, D. Prendergast, D. M. Neumark and S. R. Leone, *Nat. Commun.*, 2020, **11**, 4042.

31 H. Wu, Y. Zhou, L. Yin, C. Hang, X. Li, H. Ågren, T. Yi, Q. Zhang and L. Zhu, *J. Am. Chem. Soc.*, 2017, **139**, 785–791.

32 N. Miyaura, K. Yamada and A. Suzuki, *Tetrahedron Lett.*, 1979, **20**, 3437–3440.

33 J. Gao, Q. Xiong, X. Wu, J. Deng, X. Zhang, X. Zhao, P. Deng and Z. Yu, *Commun. Chem.*, 2020, **3**, 29.

34 X. Zhang, X. Wu, S. Jiang, J. Gao, Z. Yao, J. Deng, L. Zhang and Z. Yu, *Chem. Commun.*, 2019, **55**, 7187–7190.

35 S. Jiang, X. Wu, H. Liu, J. Deng, X. Zhang, Z. Yao, Y. Zheng, B. Li and Z. Yu, *ChemPhotoChem*, 2020, **4**, 327–331.

36 S. Arumugam and V. V. Popik, *J. Am. Chem. Soc.*, 2011, **133**, 5573–5579.

37 K. Kawaoka, A. U. Khan and D. R. Kearns, *J. Chem. Phys.*, 1967, **46**, 1842–1853.

38 O. L. J. Gijzeman, F. Kaufman and G. Porter, *J. Chem. Soc., Faraday Trans. 2*, 1973, **69**, 708.

39 D. S. McClure, *J. Chem. Phys.*, 1949, **17**, 905–913.

40 S. H. Lin and R. Bersohn, *J. Chem. Phys.*, 1968, **48**, 2732–2736.

41 R. E. Kellogg and R. P. Schwenker, *J. Chem. Phys.*, 1964, **41**, 2860–2863.

42 S. K. Lower and M. A. El-Sayed, *Chem. Rev.*, 1966, **66**, 199–241.

43 J. Guo, J. Dai, X. Peng, Q. Wang, S. Wang, X. Lou, F. Xia, Z. Zhao and B. Z. Tang, *ACS Nano*, 2021, **15**, 20042–20055.

44 G. S. Hammond and P. A. Leermakers, *J. Am. Chem. Soc.*, 1962, **84**, 207–211.

45 A. Kuboyama, F. Kobayashi and S. Morokuma, *Bull. Chem. Soc. Jpn.*, 1975, **48**, 2145–2148.

46 D. E. Nicodem, R. S. Silva, D. M. Togashi and M. F. V. da Cunha, *J. Photochem. Photobiol., A*, 2005, **175**, 154–158.

47 Y. Zhao and D. G. Truhlar, *Theor. Chem. Acc.*, 2008, **120**, 215–241.

48 R. Ditchfield, W. J. Hehre and J. A. Pople, *J. Chem. Phys.*, 1971, **54**, 724–728.

49 T. H. Dunning, *J. Chem. Phys.*, 1989, **90**, 1007–1023.

50 F. Weigend and R. Ahlrichs, *Phys. Chem. Chem. Phys.*, 2005, **7**, 3297–3305.

51 J.-D. Chai and M. Head-Gordon, *Phys. Chem. Chem. Phys.*, 2008, **10**, 6615–6620.

52 H. S. Yu, X. He, S. L. Li and D. G. Truhlar, *Chem. Sci.*, 2016, **7**, 5032–5051.

53 R. S. Silva and D. E. Nicodem, *J. Photochem. Photobiol., A*, 2004, **162**, 231–238.

54 Y. Fu, G. Alachouzos, N. A. Simeth, M. Di Donato, M. F. Hilbers, W. J. Buma, W. Szymanski and B. L. Feringa, submitted.

55 M. A. El-Sayed, *J. Chem. Phys.*, 1963, **38**, 2834–2838.